

Sensors

A Highly Fluorescent Metallosalalen-Based Chiral Cage for Enantioselective Recognition and Sensing

Jinqiao Dong, Yanfang Zhou, Fangwei Zhang, and Yong Cui*^[a]

Abstract: A highly fluorescent coordination cage $[Zn_8L_4Cl_8]$ has been constructed by treating enantiopure pyridyl-functionalized metallosalalen units (L) with zinc(II) iodide and characterized by a variety of techniques including microanalysis, thermogravimetric analysis (TGA), circular dichroism (CD) spectroscopy, and single-crystal and powder X-ray diffraction. Strong intermolecular π - π , $CH\cdots\pi$, and $CH\cdots I$ interactions direct packing of the cage molecules to generate a 3D polycage network interconnected by pentahedral cages formed by adjacent pentamers. The cage has an amphiphilic helical cavity decorated with chiral NH functionalities capa-

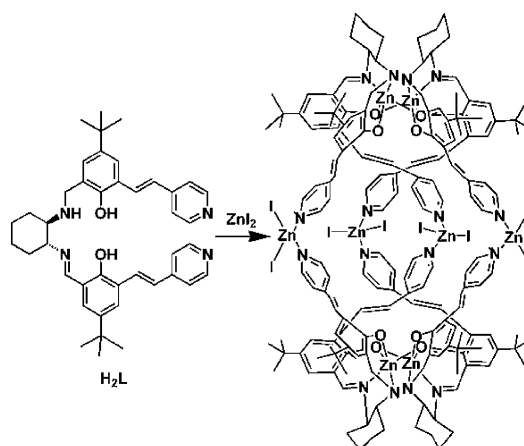
ble of interactions with guest species such as saccharides. The fluorescence of the cage was greatly enhanced by five enantiomeric saccharides in solution, with enantioselectivity factors of 2.480–4.943, and by five enantiomeric amines in the solid state, with enantioselective fluorescence enhancement ratios of 1.30–3.60. This remarkable chiral sensing of both saccharides and amines with impressive enantioselectivity may result from the steric confinement of the cavity as well as its conformational rigidity. It holds great promise for the development of novel chiral cage materials for sensing applications.

Introduction

Metal-organic containers have been extensively pursued owing to their relative ease of synthesis and potential applications in host-guest chemistry, catalysis, and sensing.^[1,2] Coordination cages with specified stereochemistry may, in principle, provide chirotopic inner phases for stereoselective guest recognition, sensing, and asymmetric transformation, as a result of their unique chemical environments and the confinement effect exerted by their well-defined central cavities.^[3] While many chiral cages of both metal-organic and organic types have already been described, systems possessing well-defined chiral functional sites that have the ability to induce enantioselectivity remain limited.^[4-6] Reports on enantioselective reactions, chiral recognition, and sensing with chiral cages are even more limited.^[5,6]

The potential application of enantioselective fluorescent sensors in rapid chiral assay has attracted significant research activity in this area.^[7] Although many enantioselective fluorescent hosts have been developed for chiral substrates such as carboxylic acids, amino acids, amines, and amino alcohols,^[8,9] relatively few have the ability to detect biologically important substrates such as saccharides.^[10] We recently reported a chiral heli-

cate cage $[Zn_8L^0_4Cl_8]$ (**2**) built from a Zn(salan) complex ($H_2L^0 = N,N'$ -bis(3-*tert*-butyl-5-(4-pyridyl)salicylidene)-1,2-diaminocyclohexane). This salan-based cage displayed enantioselective fluorescence upon interaction with amino acids,^[5g] but failed to detect saccharides. The salan ligand is saturated at the nitrogen centers and could be partially or completely oxidized to salalen and salen, respectively.^[11] We envisaged that oxidation of cage **2** to a salalen-based analogue might improve its fluorescent discriminating behavior, such that it might be applicable for recognizing saccharides.^[10] We report here the assembly of a chiral helicate cage from the salalen ligand H_2L and ZnI_2 (Scheme 1) and the first observation of enantioselective luminescence sensing of saccharides in solution and amines in the solid state by a coordination cage.



Scheme 1. The assembly of cage 1.

[a] J. Dong, Y. Zhou, F. Zhang, Prof. Y. Cui
School of Chemistry and Chemical Technology and
State Key Laboratory of Metal Matrix Composites
Shanghai Jiao Tong University
Shanghai 200240 (P.R. China)
Fax: (+86) 21-5474-1297
E-mail: yongcui@sjtu.edu.cn

Supporting information for this article is available on the WWW under
<http://dx.doi.org/10.1002/chem.201304606>.

Results and Discussion

Synthetic considerations and spectroscopic characterization

The ligand H₂L was prepared in an overall 68.2% yield by the Schiff-base condensation of 5-*tert*-butyl-3-(4-vinylpyridyl)salicylaldehyde and enantiopure 1,2-cyclohexanediamine mono-(hydrogen chloride), followed by reduction with NaBH₄ and further condensation with 5-*tert*-butyl-3-(4-vinylpyridyl)salicylaldehyde. Heating H₂L and ZnI₂ (1:2 molar ratio) in a mixed solvent of acetone and MeOH afforded [Zn₈L₄]₈·4 MeOH·4 H₂O (**1**) in good yield. The formulation was supported by the results of microanalysis, ¹H NMR, ESI-MS, and thermogravimetry (TGA).

The ¹H NMR spectrum of (*R*)-**1** displays one complete set of proton resonances for the ligand H₂L, as evidenced by two sets of signals for the *tert*-butyl groups at δ = 1.27 and 1.25 ppm. The peaks attributable to the CH₂-N groups of the coordinated ligand appear at δ = 3.79–4.07 ppm and the CH=N peak appears at δ = 8.40 ppm, confirming the partial oxidation of the imine bonds. In comparison with those of H₂L, the proton signals due to the cyclohexane units show downfield shifts, while those of the pyridyl and phenyl groups show upfield shifts, suggesting unsymmetrical coordination behavior of the ligand. All of the proton signals are very sharp, consistent with the formation of discrete metal complexes rather than oligomeric species. The formation of the cage structure was also supported by ESI-MS, which showed fragment ions [Zn₈L₄]₈+5 THF+2 H⁺, [Zn₈L₄]₈+5 THF+H+NH₄²⁺, [Zn₈L₄]₈+5 THF+Na+NH₄²⁺, and [Zn₄L₄+NH₄]⁺ at m/z = 2225.8, 2232.1, 2244.9, and 1425.4, respectively. Assembly of the cage was accompanied by amplification of the molar optical rotation. The molar optical rotation (ϕ) values of (*R*)-**1** and (*R*)-H₂L were determined as 27 500.0° cm³ dm⁻¹ mol⁻¹ and 996.7° cm³ dm⁻¹ mol⁻¹, respectively. The cage has an optical rotation per mole of 27.6 times (ca. 7 times per ligand unit) that of the ligand H₂L.

Structural description

The formation of a cage with wide apertures was revealed by single-crystal X-ray diffraction analysis.^[12] (*R*)-**1** crystallizes in the chiral tetragonal *P*₄₁₂₁ space group, with the asymmetric unit containing half a formula unit. The basic building unit is a Zn₂L₂ dimer, in which two trigonal-bipyramidal Zn centers are enclosed in the N₂O₂ pockets and linked by two phenolato oxygen atoms generating a coplanar Zn₂O₂ unit. The bond lengths and angles of the structures are typical of the salen and salen structural motifs. In particular, the Zn-N_{imine} distance [2.061(10) Å] is considerably shorter than the Zn-N_{amine} distance [2.151(10) Å]. The Zn₂L₂ dimer adopts a skewed U-shape, with the four pyridyl groups oriented towards the same face of the Zn₂O₂ plane and pointing away from the adjacent units (maximum distance between respective N atoms of around 11.0 Å). A pair of Zn₂L₂ dimers is connected through the peripheral pyridyl groups by binding to four Zn centers to generate an octanuclear cage that contains four *P*-configured quadruple-stranded helices. Each of the four Zn²⁺ ions is further coordinated by

two I⁻ ions forming a tetrahedral geometry. The cavity of the cage has inner dimensions of around 13.7×6.4 Å. The helical structure of **1** is similar to that of the un-oxidized cage **2**.

Strong intermolecular π - π , CH \cdots π , and CH \cdots I interactions direct the packing of the cage molecules into a porous 3D structure (Figure 1 b). Specifically, distorted pentahedral cages

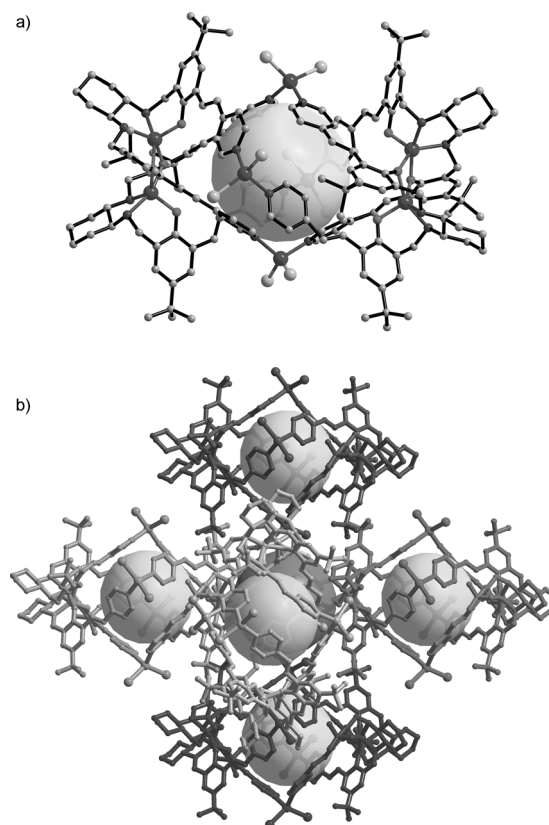


Figure 1. a) View of the molecular structure of (*R*)-**1**; b) the 3D supramolecular structure of (*R*)-**1** showing helicate cages interconnected by pentahedral cages. The cavities are shown with large spheres.

with a maximum inner width of around 8 Å are formed by the stacking of adjacent pentamers. The chiral coordinated amine groups of L are oriented toward the outside of the cages and are exposed to the interstitial pores that are accessible to guest molecules, which offers great potential for enantioselective host-guest interactions. Notably, the supramolecular engineering of porous solids from intrinsically porous assemblies is of significance but remains challenging.

Solid-state CD spectra of **1** (Figure 2) prepared from the (*R*)- and (*S*)-enantiomers of L are mirror images of one another, indicative of their enantiomeric nature. PLATON calculations indicated the presence of 27.8% void space in **1**.^[13] The phase purity of the bulk samples was established by comparison of their observed and simulated powder X-ray diffraction (PXRD) patterns. TGA revealed that the solvent molecules were removed from **1** in the range 90–160 °C. PXRD experiments suggested that the sample retained its structural integrity and crystallinity upon removal of the guest molecules. The N₂ ad-

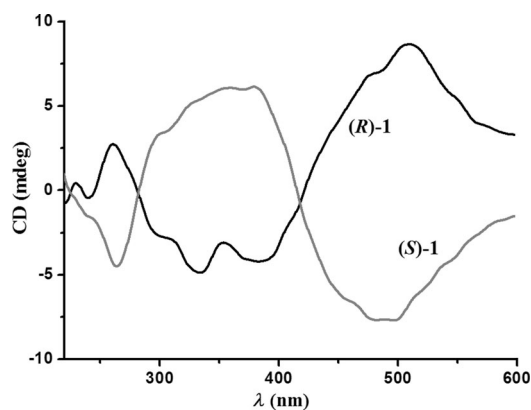
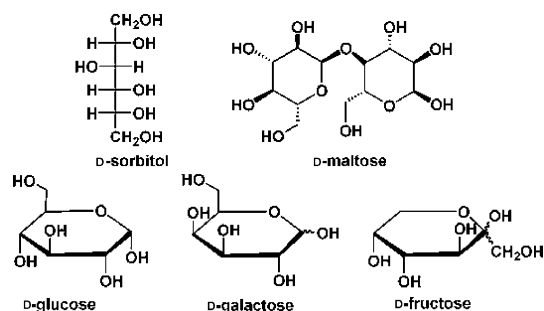


Figure 2. Solid-state CD spectra of (R)/(S)-1.

sorption isotherm at 77 K revealed that **1** showed type I sorption behavior, with a BET surface area of $25.5 \text{ m}^2 \text{ g}^{-1}$.

Fluorescence-based sensor

The fluorescence of **1** shows a strong emission at $\lambda = 530 \text{ nm}$ in THF. Compared with that of the salan-based cage analogue **2**, the emission position of **1** is little changed (530 vs 534 nm), but the intensity shows a twofold increase. Moreover, the quantum yield increased from 5.60% to 7.29% and the fluorescence lifetime from 1.615 ns to 3.622 ns. We then proceeded to investigate the interaction of the two chiral forms of **1** bearing chiral NH groups with a variety of sugars (Scheme 2). The



Scheme 2. Sugars used in the study.

results for titrations of (R)- and (S)-1 with D-sorbitol are shown in Figure 3. When **1** was treated with D-sorbitol, the emission at 530 nm was shifted to 520 nm and enhanced by the sugar, but the rate of change with (S)-1 was faster than that with (R)-1, implying enantioselectivity in the fluorescent recognition. In accordance with the linear Benesi–Hildebrand equation, the measured absorbance $[I_0/(I-I_0)]$ at 530 nm varied as a function of $1/[M]$ in a linear relationship ($R > 0.9900$), indicating 1:1 stoichiometry of the interaction between the sugar and cage **1**. The association constants K_{bh} were calculated as 4424.8 M^{-1} with (S)-1 and 895.1 M^{-1} with (R)-1, giving an enantioselectivity factor $k_{bh(S-1)}/k_{bh(R-1)}$ of $4.943 \pm 0.241:1$. After the titration, the quantum yield of **1** increased from 7.29% to 16.34%, while the

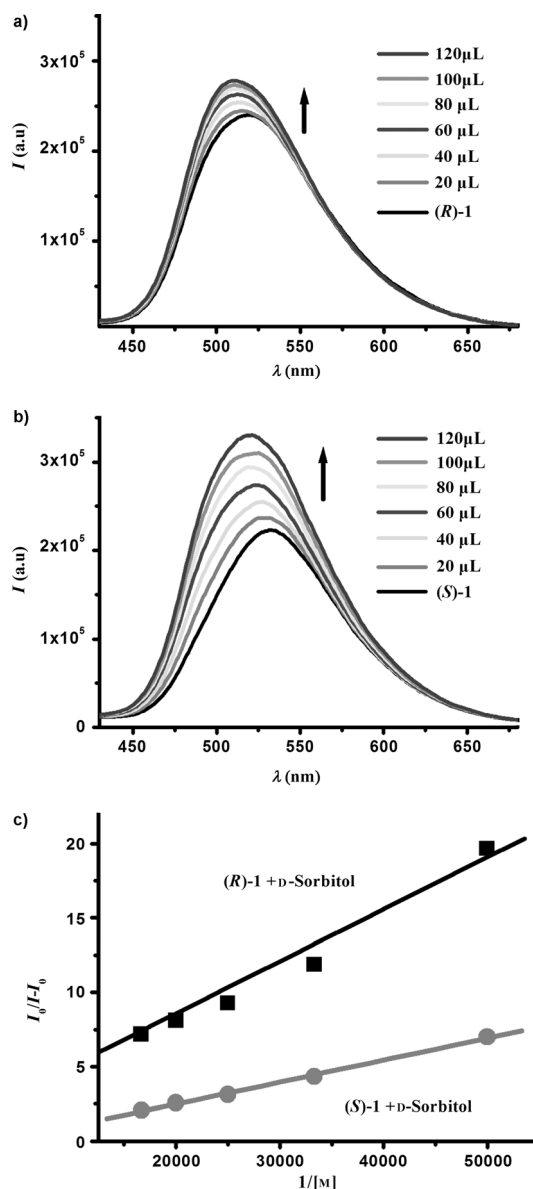


Figure 3. a, b) Fluorescence spectra of (R)- and (S)-1 ($1.0 \times 10^{-5} \text{ M}$ in THF) upon titration with D-sorbitol ($1 \times 10^{-3} \text{ M}$); c) Benesi–Hildebrand plots of (R)- and (S)-1 titration with D-sorbitol.

fluorescence lifetime of 3.533 ns remained almost unchanged. Control experiments showed that no obvious enantioselectivity was observed for the ligand H_2L , suggesting a better-defined chiral environment conferred by the cage structure. In sharp contrast, under identical experimental conditions, the addition of D-sorbitol to a solution of (R)- or (S)-2 in THF caused only a slight enhancement in the fluorescence intensity with negligible enantioselectivity (Figure S19).

The increase in fluorescence may be due to static enhancement upon formation of a cage–saccharide adduct. Changes in the structure of the emitting species, such as rigidification of the conformation, may be induced, along with excimer formation.^[14] The weak interactions of **1** with a sugar generate different diastereomeric adducts, thereby leading to a distinct fluo-

rescence enhancement. The static nature of the complexation is indicated by consistent fluorescence lifetimes of the cage before and after titration with D-sorbitol (3.622 vs 3.533 ns). After the titration, the peak position and shape of the UV/Vis spectrum of (*R*)-1 remained unchanged, indicative of the stability of the host structure. The complexation of 1 and D-sorbitol was also reflected in the ¹H NMR spectra (the proton signals of cyclohexane and the CH₂-N units of the cage were broadened after the addition of D-sorbitol).

This cage system is enantioselective towards a range of saccharides, including D-glucose, D-fructose, D-galactose, and D-maltose. The rates of fluorescence increase for (*S*)-1 caused by D-glucose and D-fructose were slower than those for (*R*)-1, whereas the rates caused by D-galactose and D-maltose were faster for (*S*)-1 than those for (*R*)-1. Their enantioselectivity factors $k_{bh(S-1)}/k_{bh(R-1)}$ were determined as 1:3.493 ± 0.101, 1:4.380 ± 0.196, 2.480 ± 0.144:1, and 4.176 ± 0.225:1, respectively. The enantio-differentiation reversal may originate from different binding affinities between the hosts and guests induced by specific intermolecular interactions, resembling the stereocontrol of an enzyme pocket in enzymatic recognition.^[15,16] The opposite trend in enantioselectivity was observed for the fluorescence enhancement of (*R*)- and (*S*)-1 by L-glucose with an enantioselectivity factor $k_{bh(S-1)}/k_{bh(R-1)}$ of 3.961 ± 0.172:1, which further confirmed a chirality-based luminescence-enhancing selectivity. The values of the enantioselectivity factors for the examined sugar alcohols are of the same order of magnitude as those obtained for sugar acids with binol-bisboronic-acid-based fluorescence sensors, although the latter exhibit lower selectivity for sugar alcohols.^[10] To the best of our knowledge, no metal-organic assemblies, such as helicates, macrocycles, or cages, have previously been reported to enantioselectively recognize saccharides.^[5,6,17]

Cage 1 is also highly fluorescent in the solid state, with an emission maximum at 610 nm and a short emission lifetime (<3 ns). Solid 1 was found to exhibit fluorescence enantioselectivity towards chiral amines. The fluorescence spectra of thin-layer samples were monitored upon exposure to the vapors of chiral molecules for various durations. When (*R*)-1 was exposed to 1-cyclohexylethylamine (1-CEA) vapor, the emission at 610 nm was shifted to 565 nm and enhanced by both the (*R*)- and (*S*)-enantiomers, but the rate of increase caused by (*R*)-1-CEA was faster than that caused by (*S*)-1-CEA (Figure 4). The enhancement percentage (%) was estimated using the formula $(I-I_0)/I_0 \times 100\%$, where I_0 is the maximum fluorescence intensity of cage 1 before exposure to the analyte, and I is the maximum intensity after exposure to the analyte. The enhancement percentages of (*R*)- and (*S*)-1-CEA were determined as 482% and 134% after 450 s, respectively. The fluorescence intensity ratio (I/I_0) of (*R*)-1 was maximally increased to 5.72 and 2.31 times that of the original value by (*R*)- and (*S*)-1-CEA, respectively, after 450 s, with an enantioselective fluorescence enhancement ratio [EF = $(I_R/I_0 - 1)/(I_S/I_0 - 1)$] of 3.60. Control experiments verified that solid H₂L showed no obvious fluorescence change in the presence of 1-CEA and no enantioselectivity. Notably, under otherwise identical conditions, the I/I_0 ratio of the salan-based cage (*R*)-2 was maximally increased

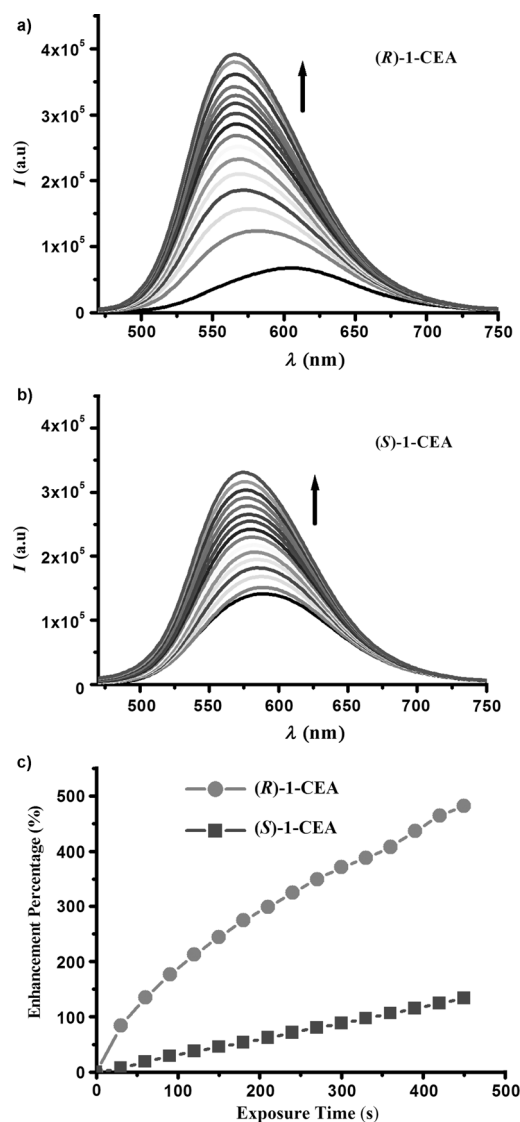


Figure 4. a, b) Fluorescence enhancement upon exposure of thin films of (*R*)-1 to vapors of (*R*)- and (*S*)-1-CEA; c) time-dependent fluorescence enhancement of (*R*)-1 by (*R*)- and (*S*)-1-CEA.

to 1.86 and 1.72 by (*R*)- and (*S*)-1-CEA, respectively, with an EF of 1.19, much smaller than that observed for (*R*)-1 (Figure S29).

Significant enantioselective fluorescence enhancements of (*R*)-1 with other chiral amines, including 1-phenylethylamine (1-PEA), 1-phenylpropylamine (1-PPA), 1-(4-methylphenyl)ethylamine (4-Me-1-PEA), and 1-(4-chlorophenyl)ethylamine (4-Cl-1-PEA), were also observed. In all cases, the rate of increase caused by the (*R*)-enantiomer was much faster than that caused by the (*S*)-enantiomer (Figure 5). The EF values were determined as 2.87, 1.32, 1.30, and 1.89 for 1-PEA, 1-PPA, 4-Me-1-PEA, and 4-Cl-1-PEA, respectively. The enantioselectivity decreases in the order 1-CEA > 1-PEA > 4-Cl-1-PEA > 1-PPA ≈ 4-Me-1-PEA.

Association of the analyte with the salalen ligand in the ground state through hydrogen bonding followed by the formation of an excellent emissive proton-transfer-assisted charge-transfer excited state may be responsible for the fluo-

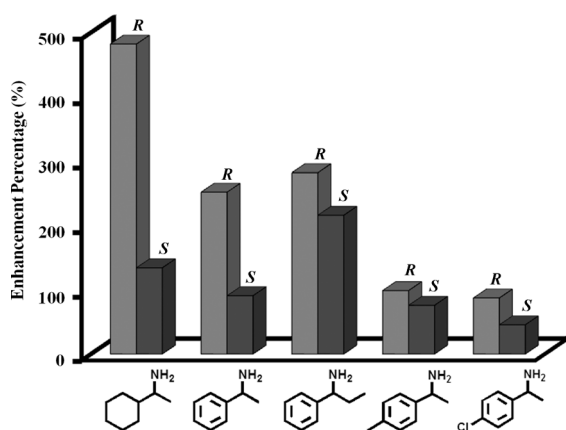


Figure 5. Maximum enhancement percentages of (*R*)-1 after exposure to chiral amines.

rescence enhancement.^[14,18] Time-resolved fluorescence measurements of **1** after addition of the amine showed only a slight decrease in the decay rate, consistent with the above fluorescence-enhancing mechanism. We propose that the enantioselective enhancement is due to the formation of different diastereomeric host-guest complexes by selective adsorption. To test this, we soaked evacuated crystals of (*R*)-**1** in solutions of racemic 1-CEA, 1-PEA, 4-Cl-1-PEA, 1-PPA, and 4-Me-1-PEA in diethyl ether. Chiral HPLC analysis of the desorbed guests from (*R*)-**1** yielded 38.5%, 17.1%, 15.7%, 12.6%, and 10.8% *ee*, respectively, with the (*R*)-enantiomers being in excess. This result is consistent with the order of decreasing selectivity from 1-CEA to 4-Me-1-PEA in fluorescence enhancement. The steric confinement of the cage creates a more discriminating chiral environment for L, leading to enhanced enantioselectivity. The conformational rigidity of the coordinated salalen ligand may also contribute to the enantioselectivity, which would reduce the non-enantioselective entropic term of the analyte association process and allow more stereospecific generation of host-guest adducts. Further study on this selective behavior and understanding the process is still in progress.

After each measurement, (*R*)-**1** could be regenerated by heating at 100 °C in vacuo for about 30 min and directly reused for a second cycle of sensing 1-CEA without significant loss of enantioselectivity (*EF* = 3.06, 3.01, 2.92 for runs 1–3, respectively). PXRD analysis showed that the sample of (*R*)-**1** remained highly crystalline after three cycles. The decrease in fluorescence intensities of (*R*)-**1** in the recycling process is believed to be due to incomplete removal of the adsorbed amines during re-activation. An alternative approach for recycling **1** is to recrystallize the sample from THF. Although metal-organic solids for sensory applications have been reported,^[19] to the best of our knowledge there has only been one report on chiral sensing (amino alcohols).^[20]

Conclusion

We have presented the assembly of a chiral helicate cage from metallosalalen that could be packed through strong supra-

molecular interactions to generate a 3D polycage network interconnected by pentahedral cages formed by adjacent pentamers. Owing to the steric confinement of the amphiphilic helical cavity together with the conformational rigidity, the chiral cage is capable of enantioselective recognition of the enantiomers of saccharides and amines through fluorescence enhancement in solution and the solid state, respectively. The amplified chiral discrimination of analytes afforded by the rigid cage structure may be utilized to design assembled materials with practical enantioselectivity for sensing applications.

Experimental Section

Chemicals, reagents, and analyses

All chemicals were obtained commercially and were used without further purification. Elemental analyses of C, H, and N were performed with an EA1110 CHNS-0 CE elemental analyzer. IR spectra were recorded from samples in KBr pellets in the region 400–4000 cm⁻¹ on a Nicolet Magna 750 FTIR spectrometer. Solid-state CD spectra were recorded on a J-800 spectropolarimeter (JASCO, Japan). Thermogravimetric analyses (TGA) were carried out in an air atmosphere at a heating rate of 20 °C min⁻¹ on a STA449C integration thermal analyzer. Powder X-ray diffraction (PXRD) data were collected on a DMAX2500 diffractometer using Cu_{Kα} radiation. Calculated PXRD patterns were produced using the SHELXTL-XPOW program and single-crystal reflection data. All UV/Vis absorption spectra were recorded on a Lambda 20 UV/Vis spectrophotometer (Perkin-Elmer, Inc., USA). Fluorescence spectra were recorded on an LS 50B fluorescence spectrometer (Perkin-Elmer, Inc., USA). Fluorescence lifetimes were measured with an Edinburgh Instruments lifspec-red F900 fluorescence lifetime spectrometer. ¹H and ¹³C NMR experiments were carried out on a Mercury plus 400 spectrometer operating at resonance frequencies of 400 MHz and 100 MHz, respectively. Electrospray ionization mass spectra (ESI-MS) were recorded on a Finnigan LCQ mass spectrometer using dichloromethane/methanol as the mobile phase. Analytical high-performance liquid chromatography (HPLC) was performed on a YL-9100 HPLC with UV detection at 254 nm. Analytical Chiralcel OD-H columns (4.6 mm × 25 cm) from Daicel were used.

X-ray crystallography

Single-crystal XRD data for (*R*)-**1** were collected on a Bruker SMART Apex II CCD-based X-ray diffractometer with Cu_{Kα} radiation ($\lambda = 1.54178 \text{ \AA}$) at 123 K. An empirical absorption correction was applied by using the SADABS program (G. M. Sheldrick, SADABS, Program for empirical absorption correction of area detector data; University of Göttingen, Germany, 1996). All structures were solved by direct methods and refined by full-matrix least-squares on F^2 (G. M. Sheldrick, SHELXTL97, Program for crystal structure refinement, University of Göttingen, Germany, 1997). In all compounds, the guest molecules and H atoms were refined isotropically, while all other atoms were refined anisotropically. All phenyl rings were constrained to ideal six-membered rings. Contributions to scattering due to the highly disordered solvent molecules in (*R*)-**1** were removed using the SQUEEZE routine of PLATON; structures were then refined once more using the data generated. Crystal data and details of the data collection are given in Table S1. Selected bond distances and angles are presented in Table S2.

Synthesis of 1

A mixture of ZnI_2 (31.9 mg, 0.1 mmol), (*R*)- H_2L or (*S*)- H_2L (32.1 mg, 0.05 mmol), acetone (5 mL), and MeOH (5 mL) was sealed in a 10 mL vial with a screw-cap and heated at 65 °C for 2 days. The mixture was then cooled to room temperature, whereupon light-yellow block-shaped crystals were collected, washed with diethyl ether, and dried in air. Yield: 38.9 mg, 76.0%. Elemental analysis calcd (%) for $[Zn_8L_4] \cdot 4MeOH \cdot 4H_2O$ ($C_{172}H_{220}I_8N_{16}O_{16}Zn_8$): C 47.98, H 5.11, N 5.21; found: C 47.51, H 5.08, N 5.14; IR (KBr): $\tilde{\nu} = 3443$ (m), 2950 (m), 2861 (w), 1604 (s), 1546 (w), 1501 (w), 1447 (s), 1463 (m), 1362 (w), 1285 (w), 1251 (w), 1202 (m), 1024 (m), 1229 (s), 977 (w), 874 (w), 829 (w), 774 (w), 731 (w), 539 cm^{-1} (w); 1H NMR ($[D_6]DMSO$) $\delta = 8.40$ – 8.36 (m, 3H; pyridyl-H + ArH), 8.07– 8.02 (m, 3H; pyridyl-H + ArH), 7.69– 7.52 (m, 5H; vinyl-H + ArH), 7.30– 7.03 (m, 6H; vinyl-H + pyridyl-H), 4.07– 3.79 (m, 2H; methylene-H), 3.53– 3.51 (m, 1H; cyclohexadecyl-H), 3.18– 3.15 (m, 1H; cyclohexadecyl-H), 2.47– 2.45 (m, 1H; cyclohexadecyl-H), 2.36– 2.34 (m, 1H; cyclohexadecyl-H), 1.99– 1.78 (m, 4H; cyclohexadecyl-H), 1.27– 1.25 (d, 18H; $2CMe_3$), 1.03– 1.01 ppm (m, 2H; cyclohexadecyl-H). The guest molecules could be readily removed to generate apohost (*R*)-1 by heating the pristine sample at 100 °C for 4 h. The 1H NMR spectrum was recorded from the apohost sample.

General procedures for fluorescence sensor experiments

Titration experiments were carried out by adding aliquots (20 μL) of substrate solution ($1.0 \times 10^{-3} mol L^{-1}$) to a solution of (*R*)- or (*S*)-1 ($1.0 \times 10^{-5} mol L^{-1}$) in THF (2 mL) at intervals of 5 min. Fluorescence spectra were recorded after addition of the substrate. The excitation wavelength was 350 nm and the slit width was set at 4 nm \times 4 nm.

For solid-state experiments, apohost cage 1 was ground to a powder and sprinkled evenly and firmly onto the surface of double-sided tape and then applied to the lower half of a quartz slide (on either side). In this way, thin-layer samples of quartz slides bearing cage 1 were obtained, which were placed in quartz cuvettes saturated with analyte vapor and the temporal evolution of the fluorescence spectra was monitored.^[19b] The excitation wavelength was 380 nm and the slit width was set at 4 nm \times 4 nm.

General procedure for adsorption separation and chiral HPLC analysis of resolved substrates by (*R*)-1

Racemic 1-cyclohexylethylamine (25.4 mg, 0.2 mmol), 1-phenylethylamine (24.2 mg, 0.2 mmol), 1-phenylpropylamine (27.0 mg, 0.2 mmol), 1-(4-methylphenyl)ethylamine (27.0 mg, 0.2 mmol), and 1-(4-chlorophenyl)ethylamine (31.1 mg, 0.2 mmol) were separately added to suspensions of the apohost (*R*)-1 (82.0 mg, 0.02 mmol) in dry Et_2O . The resulting suspensions were kept at -10 °C for 3 days, and then the solids were collected by filtration and washed with Et_2O to remove surface guest molecules. The guest molecules could be readily removed from the inclusion solids by soaking in Et_2O . Et_3N (1 drop) and $BzCl$ (1 drop) were added to a solution of the encapsulated amine in Et_2O (5 mL) at room temperature. The resulting reaction mixture was stirred for 4 h, then diluted with Et_2O (5 mL), washed with aqueous HCl (1 M, 2 mL) and saturated NaCl solution, dried over anhydrous Na_2SO_4 , and concentrated in vacuo. The optical purity of the benzoylated amine was then analyzed by HPLC determination on a Chiralcel OD-H column (4.6 mm \times 25 cm).

The enantiomeric excess of 1-cyclohexylethylamine was determined by benzoylation followed by HPLC analysis. Conditions:

Chiralcel OD-H column: 25 °C; hexane/*i*PrOH (95:5); flow rate 1.0 mL min^{-1} ; $t_{major} = 10.850$ min, $t_{min} = 20.583$ min; ee = 38.5%.

The enantiomeric excess of 1-phenylethylamine was determined by benzoylation followed by HPLC analysis. Conditions: Chiralcel OD-H column: 25 °C; hexane/*i*PrOH (90:10); flow rate 1.0 mL min^{-1} ; $t_{major} = 12.833$ min, $t_{min} = 19.183$ min; ee = 17.1%.

The enantiomeric excess of 1-(4-chlorophenyl)ethylamine was determined by benzoylation followed by HPLC analysis. Conditions: Chiralcel OD-H column: 25 °C; hexane/*i*PrOH (90:10); flow rate 1.0 mL min^{-1} ; $t_{major} = 12.250$ min, $t_{min} = 21.267$ min; ee = 15.7%.

The enantiomeric excess of 1-phenylpropylamine was determined by benzoylation followed by HPLC analysis. Conditions: Chiralcel OD-H column: 25 °C; hexane/*i*PrOH (95:5); flow rate 1.0 mL min^{-1} ; $t_{major} = 16.967$ min, $t_{min} = 30.483$ min; ee = 12.6%.

The enantiomeric excess of 1-(4-methylphenyl)ethylamine was determined by benzoylation followed by HPLC analysis. Conditions: Chiralcel OD-H column: 25 °C; hexane/*i*PrOH (95:5); flow rate 1.0 mL min^{-1} ; $t_{major} = 17.017$ min, $t_{min} = 32.017$ min; ee = 10.8%.

Acknowledgements

This work was supported by the NSFC through grants 21025103 and 21371119, the "973" program (2014CB932102 and 2012CB8217), and the Shanghai Science and Technology Committee through grant 10J1400100.

Keywords: chirality · coordination cage · fluorescence sensor · metal–organic frameworks · metallosalalen · saccharides

- [1] a) R. Chakrabarty, P. S. Mukherjee, P. J. Stang, *Chem. Rev.* **2011**, *111*, 6810; b) M. D. Ward, *Chem. Commun.* **2009**, 4487; c) T. S. Koblenz, J. Wassenaar, J. N. H. Reek, *Chem. Soc. Rev.* **2008**, *37*, 247; d) R. W. Saalfrank, H. Maid, A. Scheurer, *Angew. Chem.* **2008**, *120*, 8924; *Angew. Chem. Int. Ed.* **2008**, *47*, 8794; e) M. Fujita, M. Tominaga, A. Hori, B. Therrien, *Acc. Chem. Res.* **2005**, *38*, 369; f) P. Jin, S. J. Dalgarno, J. L. Atwood, *Coord. Chem. Rev.* **2010**, *254*, 1760; g) H. Amouri, C. Desmarets, J. Moussa, *Chem. Rev.* **2012**, *112*, 2015.
- [2] a) M. D. Pluth, R. G. Bergman, K. N. Raymond, *Science* **2007**, *316*, 85; b) P. Mal, B. Breiner, K. Rissanen, J. R. Nitschke, *Science* **2009**, *324*, 1697; c) M. Kuil, T. Soltner, P. W. N. M. Van Leeuwen, J. N. H. Reek, *J. Am. Chem. Soc.* **2006**, *128*, 11344; d) Q. Sun, J. Iwasa, D. Ogawa, Y. Ishido, S. Sato, T. Ozeki, Y. Sei, K. Yamaguchi, M. Fujita, *Science* **2010**, *328*, 1144; e) H. Ito, M. Ikeda, T. Hasegawa, Y. Furusho, E. Yashima, *J. Am. Chem. Soc.* **2011**, *133*, 3419; f) E. Yashima, K. Maeda, Y. Furusho, *Acc. Chem. Res.* **2008**, *41*, 1166; g) W. Meng, J. K. Clegg, J. D. Thoburn, J. R. Nitschke, *J. Am. Chem. Soc.* **2011**, *133*, 13652; h) J. F. Ayme, J. E. Beves, D. A. Leigh, R. T. McBurney, K. Rissanen, D. Schultz, *Nat. Chem.* **2012**, *4*, 15; i) B. Birkmann, R. Frölich, F. E. Hahn, *Chem. Eur. J.* **2009**, *15*, 9325; j) K. Allen, R. Faulkner, L. Harding, C. Rice, T. Riis-Johannessen, M. Voss, M. Whitehead, *Angew. Chem.* **2010**, *122*, 6805; *Angew. Chem. Int. Ed.* **2010**, *49*, 6655.
- [3] a) M. D. Pluth, R. G. Bergman, K. N. Raymond, *Acc. Chem. Res.* **2009**, *42*, 1650; b) M. M. J. Smulders, I. A. Riddell, C. Browne, J. R. Nitschke, *Chem. Soc. Rev.* **2013**, *42*, 1728; c) T. D. Hamilton, L. R. MacGillivray, *Cryst. Growth Des.* **2004**, *4*, 419.
- [4] a) Y. Nishioka, T. Yamaguchi, M. Kawano, M. Fujita, *J. Am. Chem. Soc.* **2008**, *130*, 8160; b) S. P. Argent, T. Riis-Johannessen, J. C. Jeffery, L. P. Harding, M. D. Ward, *Chem. Commun.* **2005**, 4647; c) N. Ousaka, J. K. Clegg, J. R. Nitschke, *Angew. Chem.* **2012**, *124*, 1493; *Angew. Chem. Int. Ed.* **2012**, *51*, 1464; d) N. Ousaka, S. Grunder, A. M. Castilla, A. C. Whalley, J. F. Stoddart, J. R. Nitschke, *J. Am. Chem. Soc.* **2012**, *134*, 15528.
- [5] a) M. Ziegler, A. V. Davis, D. W. Johnson, K. N. Raymond, *Angew. Chem.* **2003**, *115*, 689; *Angew. Chem. Int. Ed.* **2003**, *42*, 665; b) D. H. Leung, R. G. Bergman, K. N. Raymond, *J. Am. Chem. Soc.* **2006**, *128*, 9781; c) A. Nakamura, Y. Inoue, *J. Am. Chem. Soc.* **2005**, *127*, 5338; d) A. V. Davis, D. Fie-

- dler, M. Ziegler, A. Terpin, K. N. Raymond, *J. Am. Chem. Soc.* **2007**, *129*, 15354; e) D. Fiedler, D. H. Leung, R. G. Bergman, K. N. Raymond, *J. Am. Chem. Soc.* **2004**, *126*, 3674; f) T. Liu, Y. Liu, W. Xuan, Y. Cui, *Angew. Chem.* **2010**, *122*, 4215; *Angew. Chem. Int. Ed.* **2010**, *49*, 4121; g) W. Xuan, M. Zhang, Y. Liu, Z. Chen, Y. Cui, *J. Am. Chem. Soc.* **2012**, *134*, 6904.
- [6] a) J. Rebek Jr., *Acc. Chem. Res.* **2009**, *42*, 1660; b) T. Iwasawa, R. J. Hooley, J. Rebek Jr., *Science* **2007**, *317*, 493; c) R. Holst, A. Trewin, A. I. Cooper, *Nat. Chem.* **2010**, *2*, 915; d) X. J. Liu, R. Warmuth, *J. Am. Chem. Soc.* **2006**, *128*, 14120; e) Y. Z. Liu, C. H. Hu, A. Comotti, M. D. Ward, *Science* **2011**, *333*, 436; f) B. İçli, N. Christinat, J. Tonnemann, C. Schuttler, R. Scopelliti, K. Severin, *J. Am. Chem. Soc.* **2009**, *131*, 3154; g) Y. Jin, B. A. Voss, A. Jin, H. Long, R. D. Noble, W. Zhang, *J. Am. Chem. Soc.* **2011**, *133*, 6650; h) T. Kida, T. Iwamoto, H. Asahara, T. Hinoue, M. Akashi, *J. Am. Chem. Soc.* **2013**, *135*, 3371; i) J. Sun, J. L. Bennett, T. J. Emge, R. Warmuth, *J. Am. Chem. Soc.* **2011**, *133*, 3268.
- [7] a) L. Pu, *Acc. Chem. Res.* **2012**, *45*, 150; b) D. Leung, S. O. Kang, E. V. Anslyn, *Chem. Soc. Rev.* **2012**, *41*, 448; c) S. D. Bull, M. G. Davidson, J. M. H. Van Den Elsen, J. S. Fossey, A. T. A. Jenking, Y. B. Jiang, Y. Kubo, F. Marken, K. Sakural, J. Zhao, T. D. James, *Acc. Chem. Res.* **2013**, *46*, 312.
- [8] a) V. Pugh, Q. S. Hu, L. Pu, *Angew. Chem.* **2000**, *112*, 3784; *Angew. Chem. Int. Ed.* **2000**, *39*, 3638; b) G. A. Korbel, G. Lalic, M. D. Shair, *J. Am. Chem. Soc.* **2001**, *123*, 361; c) E. R. Jarvo, C. A. Evans, G. T. Copeland, S. J. Miller, *J. Org. Chem.* **2001**, *66*, 5522; d) W. L. Wong, K. H. Huang, P. F. Teng, C. S. Lee, H. L. Kwong, *Chem. Commun.* **2004**, 384; e) S. Pagliari, R. Corradini, G. Galaverna, S. Sforza, A. Dossena, M. Montalti, L. Prodi, N. Zaccaroni, R. Marchelli, *Chem. Eur. J.* **2004**, *10*, 2749; f) L. Zhu, E. V. Anslyn, *J. Am. Chem. Soc.* **2004**, *126*, 3676; g) X. F. Mei, C. Wolf, *J. Am. Chem. Soc.* **2004**, *126*, 14736; h) Z. Li, J. Lin, L. Pu, *Angew. Chem.* **2005**, *117*, 1718; *Angew. Chem. Int. Ed.* **2005**, *44*, 1690; i) S. Yu, W. Plunkett, M. Kim, L. Pu, *J. Am. Chem. Soc.* **2012**, *134*, 20282; j) S. S. Yu, L. Pu, *J. Am. Chem. Soc.* **2010**, *132*, 17698; k) X. F. Mei, C. Wolf, *J. Am. Chem. Soc.* **2006**, *128*, 13326.
- [9] a) S. J. Lee, A. Hu, W. Lin, *J. Am. Chem. Soc.* **2002**, *124*, 12948; b) J. Hua, W. Lin, *Org. Lett.* **2004**, *6*, 861; c) S. S. Sun, C. L. Stern, S. T. Nguyen, J. T. Hupp, *J. Am. Chem. Soc.* **2004**, *126*, 6314; d) M. S. Masar, N. C. Gianneschi, C. G. Oliveri, C. L. Stern, S. T. Nguyen, C. A. Mirkin, *J. Am. Chem. Soc.* **2007**, *129*, 10149; e) F. Song, G. Wei, L. Wang, J. Jiao, Y. Cheng, C. Zhu, *J. Org. Chem.* **2012**, *77*, 4759; f) V. A. Soloshonok, T. K. Ellis, H. Ueki, T. Ono, *J. Am. Chem. Soc.* **2009**, *131*, 7208; g) D. Ryu, E. Park, D. S. Kim, S. Yan, J. Y. Lee, B. Y. Chang, K. H. Ahn, *J. Am. Chem. Soc.* **2008**, *130*, 2394.
- [10] a) T. D. James, K. R. A. S. Sandanayake, S. Shinkai, *Nature* **1995**, *374*, 345; b) J. Z. Zhao, T. M. Fyles, T. D. James, *Angew. Chem.* **2004**, *116*, 3543; *Angew. Chem. Int. Ed.* **2004**, *43*, 3461; c) J. Z. Zhao, M. G. Davidson, M. F. Mahon, G. Kocio-Köhn, T. D. James, *J. Am. Chem. Soc.* **2004**, *126*, 16179; d) S. Arimori, M. L. Bell, C. S. Oh, T. D. James, *Org. Lett.* **2002**, *4*, 4249; e) J. Zhao, T. D. James, *J. Mater. Chem.* **2005**, *15*, 2896.
- [11] K. Matsumoto, B. Saito, T. Katsuki, *Chem. Commun.* **2007**, 3619.
- [12] Crystal data for **1**: tetragonal, $P4_2,2$, $a = 19.1858(9) \text{ \AA}$, $c = 60.203(3) \text{ \AA}$, $V = 22160.3(19) \text{ \AA}^3$, $D_{\text{calcd}} = 1.235 \text{ g cm}^{-3}$, $Z = 4$, $R_1 = 0.0873$ ($I > 2.0\sigma(I)$), $wR_2 = 0.2070$, $\text{GoF} = 1.071$, Flack parameter = 0.088(8). CCDC-945222 contains the supplementary crystallographic data for this paper. These data can be obtained free of charge from the Cambridge Crystallographic Data Centre via www.ccdc.cam.ac.uk/data_request/cif.
- [13] A. L. Spek, *J. Appl. Crystallogr.* **2003**, *36*, 7.
- [14] a) A. Accetta, R. Corradini, R. Marchelli, *Top. Curr. Chem.* **2011**, *300*, 175; b) A. Sytnik, D. Gormin, M. Kasha, *Proc. Natl. Acad. Sci. USA* **1994**, *91*, 11968.
- [15] a) L. Simón, J. M. Goodman, *J. Org. Chem.* **2010**, *75*, 589; b) G. A. E. Oxford, D. Dubbeldam, L. J. Broadbelt, R. Q. Snurr, *J. Mol. Catal. A* **2011**, *334*, 89.
- [16] a) A. J. Kirby, *Angew. Chem.* **1996**, *108*, 770; *Angew. Chem. Int. Ed. Engl.* **1996**, *35*, 706; b) Y. Murakami, J. i. Kikuchi, Y. Hisaeda, O. Hayashida, *Chem. Rev.* **1996**, *96*, 721.
- [17] a) T. D. James, S. Shinkai, *Top. Curr. Chem.* **2002**, *218*, 159; b) T. D. James, H. Shinmori, S. Shinkai, *Chem. Commun.* **1997**, 71; c) Y. Huang, W. Ouyang, X. Wu, Z. Li, J. S. Fossey, T. D. James, Y. Jiang, *J. Am. Chem. Soc.* **2013**, *135*, 1700.
- [18] Y. Zhou, J. Yoon, *Chem. Soc. Rev.* **2012**, *41*, 52.
- [19] a) H. Wu, Q. Gong, D. H. Olson, J. Li, *Chem. Rev.* **2012**, *112*, 836; b) S. Pramanik, C. Zheng, X. Zhang, T. J. Emge, J. Li, *J. Am. Chem. Soc.* **2011**, *133*, 4153; c) Z. Zhang, S. Xiang, X. Rao, Q. Zheng, F. R. Fronczek, G. Qian, B. Chen, *Chem. Commun.* **2010**, *46*, 7205; d) B. Gole, A. K. Bar, P. S. Mukherjee, *Chem. Commun.* **2011**, 47, 12137.
- [20] M. M. Wanderley, C. Wang, C. Wu, W. Lin, *J. Am. Chem. Soc.* **2012**, *134*, 9050.

Received: November 25, 2013
Published online on April 7, 2014